ELSEVIER

Journal of Alloys and Compounds 317–318 (2001) 320–323

Journal of ALLOYS AND COMPOUNDS

www.elsevier.com/locate/jallcom

Isothermal cross-section of the Ce–Pd–Si phase diagram at 600°C

Yu.D. Seropegin[a,*], A.V. Gribanov[a], O.L. Kubarev[a], A.I. Tursina[a], O.I. Bodak[b]

[a]*Chemistry Department, Moscow State University, Moscow 119899, GSP, V-234, Russia*
[b]*Chemistry Department, Lviv State University, Lviv 290602, Ukraine*

Abstract

The interaction of the components in the Ce–Pd–Si system at 600°C was investigated over the whole concentration range by X-ray powder and single crystal diffraction, DTA, and X-ray microprobe analysis. The formation of the two previously reported phases, $CePd_2Si$ and $Ce_2Pd_3Si_5$, was not confirmed. There are ten ternary compounds in the Ce–Pd–Si system. The crystal structures of seven of them were determined. © 2001 Published by Elsevier Science B.V.

Keywords: Rare earth compounds; Phase equilibria; Ternary system

1. Introduction

The ternary compounds RE-TM-X (*RE*=rare earth, *TM*=transition metal, *X*=Si or Ge) are known to exhibit a number of interesting properties such as heavy-fermion superconductivity, Kondo behavior, anomalous magnetism, and/or intermediate valency. Ternary system Ce–Pd–Si is notable for Kondo–lattice phase $Ce_3Pd_{20}Si_6$, which was found and studied in earlier researches [1–3]. It was established that this compound displays the unique low-temperature properties [2,3].

The aim of the present investigation was to obtain data about the interaction of the components in the Ce–Pd–Si ternary system in the whole concentration range and about the crystal structure of new ternary intermetallic compounds.

The three binary systems bounding the ternary system have been described in detail in the literature. In reference [4] the Ce–Si binary system is reported as a review of the all previous works, in which this binary system was investigated in whole concentration range by X-ray powder diffraction, DTA and metallographic analyses. Six intermediate phases were found in this work: Ce_5Si_3, Ce_3Si_2, Ce_5Si_4, CeSi, Ce_3Si_5, and $CeSi_{2-x}$. Except $CeSi_{2-x}$ all intermediate binary phases have a fixed composition. The homogeneity range of $CeSi_{2-x}$ stretches from 63.5 to 66.7 at. % Si. According to Munitz et al. [4], at 600°C, cerium and silicon do not dissolve any noticeable amount of the second component. Crystal structure and lattice parameter data for the binary phases of the Ce–Si system are summarized in Table 1 [4].

All previous reports about the interaction of the components in the Ce–Pd binary system were summarized and analyzed in the Okamoto's review [5]. There are eight intermediate phases in the Ce–Pd system [5]: Ce_7Pd_3, Ce_3Pd_2, CePd, Ce_3Pd_4, Ce_3Pd_5, $CePd_3$, $CePd_5$, $CePd_7$. Two of these, CePd and $CePd_5$, have low- and high-temperature modifications (α and β) of their of crystal structure.

At 600°C both exist in their low-temperature modifications. Palladium dissolves up to 13 at.% Ce at 1075°C. Cerium does not dissolve any noticeable amount of palladium. As derived from the X-ray powder diffraction and microstructure data, the homogeneity region of $CePd_3$ is about 1.4 at.% [5,6]. The other intermediate phases have fixed compositions. In our work the solubility of cerium in palladium at 600°C is about 9 at.%. The homogeneity regions of the other intermediate phases are in accordance with literature data. Crystal structure and lattice parameters data for the binary phases of the Ce–Pd system are summarized in Table 2 [5].

The last detailed study on Pd–Si binary phase diagram was reported in Ref. [7]. This careful experimental work took into account the previous data summarized in [8]. According to [7] at 600°C there are seven binary intermediate phases $Pd_{84}Si_{16}$, $Pd_{82.3}Si_{17.7}$, Pd_3Si, $Pd_{66.7}Si_{33.3}$, $Pd_{66.5}Si_{33.5}$, $Pd_{66.1}Si_{33.9}$, $Pd_{65.5}Si_{34.5}$ in the Pd–Si system. The crystal structures are known for Pd_3Si (Fe_3P structural type, *Pnma*, a=0.5735 nm, b=0.7555 nm c=0.5260 nm [9]) and $Pd_{66.5}Si_{33.5}$, which corresponds to earlier reported Pd_2Si (Fe_2P structural type, *P62m*, a=0.6528 nm, c=

*Corresponding author.

0925-8388/01/$ – see front matter
PII: S0925-8388(00)01422-5

Table 1
Crystal structure and lattice parameter data for the intermediate phases in the Ce–Si system [4]

Phase	Composition, at.% Si	Space group	Prototype	Lattice parameters, nm		
				a	*b*	*c*
Ce_5Si_3	37.5	*I4/mcm*	W_5Si_3	0.7868		1.373
Ce_3Si_2	40	*P4/mbm*	U_3Si_2	0.780		0.434
Ce_5Si_4	44.4	$P4_12_12$	Zr_5Si_4	0.793		1.504
CeSi	50	*Pnma*	FeB	0.8302	0.3962	0.5964
Ce_3Si_5	62.5	*Imma*	α-$GdSi_2$	0.4192	0.413	1.392
$CeSi_{2-x}$	63.5 to 66.7	$I4_1/amd$	α-$ThSi_2$	0.4192		1.390

Table 2
Crystal structure and lattice parameter data for the intermediate phases in the Ce–Pd system [5,6]

Phase	Composition, at.% Pd	Space group	Prototype	Lattice parameters, nm		
				a	*b*	*c*
Ce_7Pd_3	30	$P6_3mc$	Fe_3Th_7	1.0222		0.6441
Ce_3Pd_2	40					
α-CePd	50	*Cmcm*	CrB	0.3890	1.0910	0.4635
β-CePd	50	*Pnma*	FeB			
Ce_3Pd_{4x}	57.1	$R\bar{3}$	Pu_3Pd_4	1.3669		0.5824
Ce_3Pd_5	62.5	$P\bar{6}2m$	Th_3Pd_5			
$CePd_3$	74.8–76.2	$Pm\bar{3}m$	Cu_3Au	0.4160		
α-$CePd_5$	83.3	*Pnma*		0.5700	0.4062	0.8462
β-$CePd_5$	83.3	*cubic*		0.4055		
$CePd_7$	87.5	$Fm\bar{3}m$	Pt_7Cu	0.80805		

0.3437 nm [9]). The reciprocal solubility of Pd and Si in each other at 600°C is found to be negligible [7].

Systematic studies of the ternary Ce–Pd–Si system through the whole concentration range have not previously been performed. Up to now the following ternary intermetallic compounds were described or mentioned in the literature: $Ce_3Pd_{20}Si_6$ [1–3], $CePd_2Si_2$ [10], $CePd_2Si$ [11], and $Ce_2Pd_3Si_5$ [12].

The crystallographic data that has been published for these four phases are given in Table 3 with references.

2. Experimental details

The present investigation was done with 117 samples having masses of about 1 g. These were made in an electric arc furnace under an argon atmosphere with a nonconsumable tungsten electrode and a water cooled copper hearth. The purity of cerium was 99 at.%, the purity of palladium and silicon was better than 99.9 at.%. Titanium was used as a getter during melting. The alloys were remelted two times in order to achieve complete fusion and homogeneity. Alloys with melting losses not exceeding 1 wt.% were choosen for the experiments. After melting all alloys were subjected to a homogenizing anneal in evacuated double-walled quartz ampoules containing titanium chips as getters. Annealing was done in a resistance furnace at 600°C for 720 h with subsequent quench into ice water.

X-ray powder and monocrystal diffraction, DTA, and electron probe X-ray analyses were used in the present investigation.

Initial phase analyses were performed with an URS-60 generating unit with Cr K_α radiation (λ=0.229092 nm) for RKD-57 cameras having asymmetric film loading. For

Table 3
Crystal structure and lattice parameter data published for the ternary intermediate phases of the Ce–Pd–Si system

Phase	Space group	Prototype	Lattice parameters, nm			Ref.
			a	*b*	*c*	
$Ce_3Pd_{20}Si_6$	$Fm\bar{3}m$	$Ce_3Pd_{20}Ge_6$	1.2161			[1]
			1.2280			[2]
$CePd_2Si_2$	*I4/mmm*	$ThCu_2Si_2$	0.4232		0.9911	[10]
$CePd_2Si$	*Pnma*	YPd_2Si	0.6877	0.7609	0.5695	[11]
$Ce_2Pd_3Si_5$	*Ibam*	$U_2Co_3Si_5$				[12]

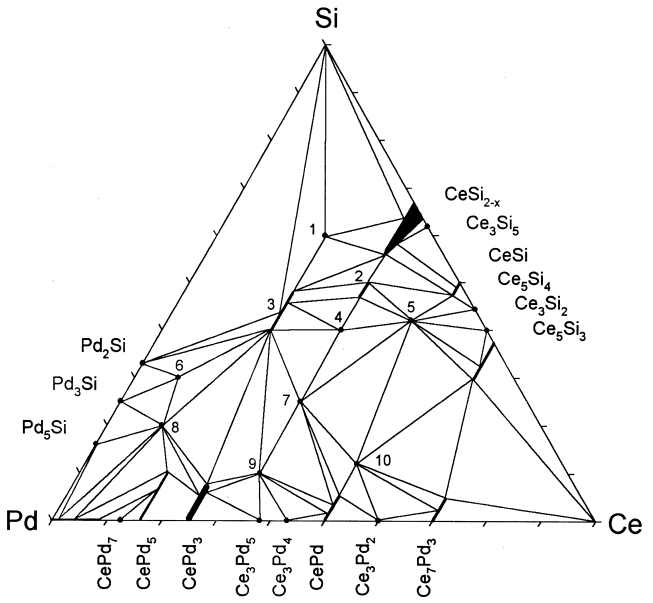

Fig. 1. Isothermal cross-section of the Ce–Pd–Si system at 600°C.

precision lattice parameters, one or the other of the following was used:

- 'DRON-2.0' with Fe K_α radiation, λ=0.193728 nm;
- 'DRON-3.0' with Cu K_α radiation, λ=0.154178 nm;
- FR-552 focusing monochromator camera with Cu $K_{\alpha 1}$ radiation, λ=0.154051 nm and Ge as an internal standard.

X-ray monocrystal analyses were first made photographically with RKV-86 camera and Mo K radiation, then with an Enraf-Nonius CAD-4 autodiffractometer and Mo K_α radiation. Calculations were performed with the CSD-programs of [13].

Electron probe X-ray analyses were done with a 'Camebax Microbeam' analyzer. This device was used for phase identification of the individual grains in the microstructure by energy dispersive analyses of secondary electrons in combination with determination of the position and intensity of characteristic X-ray wavelengths.

DTA experiments were executed on high temperature VDTA-8M_2 equipment (W-W/Re thermocouples) in BeO crucibles. As standards for the calibrating pure Fe, Cu, Pt metals were used.

3. Results and discussion

Results from the present measurements were used in the construction of the isothermal cross-section of the Ce–Pd–Si phase diagram at 600°C (Fig. 1). The ternary phases $CePd_2Si$ and $Ce_2Pd_3Si_5$ were not found in our study. $CePd_5$, $CePd_3$, CePd, Ce_7Pd_3, Ce_5Si_3, CeSi, and $CeSi_{2-x}$ all have noticeable extentions into the ternary system. The homogeneity regions of the other binary phases are negligible.

The interaction of Ce, Pd and Si leads to the formation of at least ten ternary phases stable at 600°C, including the two phases already reported (Table 4). Powder diffraction method was applied for calculating the structure of $CePdSi_3$, $CePd_2Si_2$, $Ce(Pd,Si)_2$, $Ce_4(Pd,Si)_8$, and $Ce_3Pd_{20}Si_6$. The structures of $Ce_8Pd_{62}Si_{30}$ and Ce_3Pd_5Si were determined on single crystals. Investigation of the powder diffraction data of three alloys with the approximate compositions $Ce_{45}Pd_{13}Si_{42}$, $Ce_{33}Pd_{42}Si_{25}$, and $Ce_{50}Pd_{38}Si_{12}$ leads to the speculation that even more ternary phases may exist at or near these compositions. However, no crystal structure determinations were performed because suitable single crystals were not obtained. The obtained crystallographic data are presented in Table 4.

DTA experiments show the following thermal effects on heating the following samples:

$Ce_3Pd_{20}Si_6$ 1240±5°C

Ce_3Pd_5Si $T_1 = 950\pm5$°C, $T_2 = 985\pm5$°C

Table 4
Crystal structure and lattice parameter data for the ternary intermediate phases in the Ce–Pd–Si system

N. Phase	Space group	Prototype	Lattice parameters, nm		
			a	*b*	*c*
1. $CePdSi_3$	*I4 mm*	$BaNiSn_3$	0.43209(5)		0.9606(2)
2. $Ce(Pd,Si)_2$	*P6/mmm*	AlB_2	0.4219(4)		0.4134(4)
3. $CePd_2Si_2$	*I4/mmm*	$CeAl_2Ga_2$	0.42365(7)		0.9899(3)
4. $Ce_4(Pd,Si)_8$	$I4_1/amd$	α-$ThSi_2$	0.41842(6)		1.4571(3)
5. $Ce_{45}Pd_{13}Si_{42}$					
6. $Ce_8Pd_{62}Si_{30}$[a]	$Fm\bar{3}m$		1.8010(2)		
7. $Ce_{33}Pd_{42}Si_{25}$					
8. $Ce_3Pd_{20}Si_6$	$Fm\bar{3}m$	$Ce_3Pd_{20}Ge_6$	1.2161(1)		
9. $Ce_3Pd_5Si_1$	*Imma*		1.3027(4)	0.7377(4)	0.7580(4)
10. $Ce_{50}Pd_{38}Si_{12}$					

[a] Detailed description is in press.

$Ce_8Pd_{62}Si_{30}$ $T_1 = 1110 \pm 5$°C, $T_2 = 1160 \pm 5$°C

$CePd_2Si_2$ 1510 ± 10°C

Acknowledgements

This work is supported by the Russian Foundation of Basic Research (grant N 00-03-32651a).

References

[1] A.V. Gribanov, Yu.D. Seropegin, O.I. Bodak, J. Alloys Comp. 204 (1994) L9.
[2] N. Takeda, J. Kitagawa, M. Ishikawa, J. Phys. Soc. Japan 64 (1995) 387.
[3] Yu.P. Gaidukov, Yu.A. Koksharov, Yu.B. Kochetkov et al., Lett. JETP 61 (1995) 385, in Russian.
[4] A. Munitz, A.B. Gokhale, G.J. Abbaschian, Bull. Alloy Phase Diagrams 10 (1989) 73.
[5] H. Okamoto, J. Phase Equilibria 12 (1991) 700.
[6] T. Bretschneider, H.J. Schaller, Z. Metallkunde. 81 (1990) 84.
[7] R. Massara, P. Feschotte, J. Alloys Comp. 190 (1993) 249.
[8] H.C. Baxi, T.B. Massalski, J. Phase Equilibria 12 (1991) 349.
[9] J.A. Wysocki, P.E. Duwez, Metall. Trans. A 12A (1981) 1455.
[10] D. Rossi, R. Massara, R. Ferro, J. Less-Common Metals 66 (1979) 17.
[11] J.M. Moreau, J. Le Roy, D. Paccard et al., Acta Cryst. 38 (1982) 2446.
[12] C. Godart, L.C. Gupta, C.V. Tomy et al., Mater. Res. Bull. 23 (1988) 1781.
[13] L.G. Akselrud, Yu.N. Gryn, P.Y. Zavalii, V.K. Pecharski, V.S. Fundamentsky, Twelfth European Crystallographic Meeting, Moscow, August 1989, Viniti, Moscow (1989) 155.